


Numerical study of the self-pulsing of DC discharge: from corona to parallel-plate configurations

Manqi ZHANG (张曼琦)¹, Feng HE (何锋)^{1,*}, Hongmei CAI (蔡红梅)¹,
Zeduan ZHANG (张泽端)¹, Zhiliang GAO (高志良)², Ming YANG (杨铭)²,
Ruojuan WANG (王若珏)², Yu ZHANG (张宇)², Ben LI (李犇)²,
Lei WANG (王磊)² and Jiting OUYANG (欧阳吉庭)^{1,*} 

¹ School of Physics, Beijing Institute of Technology, Beijing 100081, People's Republic of China

² Beijing Orient Institute of Measurement and Test, Beijing 100094, People's Republic of China

E-mail: hefeng@bit.edu.cn and jtouyang@bit.edu.cn

Received 11 April 2023, revised 3 July 2023

Accepted for publication 5 July 2023

Published 28 August 2023



CrossMark

Abstract

We present here an investigation of the self-pulsing phenomenon of negative corona and parallel-plate discharge in argon within one frame of a one-dimensional fluid model in cylinder-cylinder electrode geometry. The transition from corona to parallel-plate discharge is obtained by changing the inner and outer radii of the electrodes. The model reproduces the self-pulsing waveform well and provides the spatiotemporal behaviors of the charged particles and electric field during the pulse. The self-pulsing shows a common feature that occurs in various configurations and that does not depend on a specific electrode structure. The self-pulsing is the transformation between a weak-current Townsend mode and a large-current normal glow mode. The behavior of the positive ions is the dominant factor in the formation of the pulse.

Keywords: self-pulsing, mode transition, glow discharge, Townsend discharge

(Some figures may appear in colour only in the online journal)

1. Introduction

Self-pulsing is a typical instability in DC discharge in various configurations that consists of regular pulsations with short duration. The Trichel pulse in negative corona discharge is one of the most famous self-pulsing phenomena and was first discovered and named by Trichel [1]. In the early days, the Trichel pulse was believed to exist only in electronegative gases [2–4] and to be caused by the periodic accumulation and dissipation of negative ions. Several simulations of Trichel pulses have been performed for deeper exploration of their mechanism. For example, Morrow [5, 6] proposed a one-dimensional (1D) model describing the development of a Trichel pulse and investigated the spatiotemporal behaviors of the electric field and charged particles in the first pulse. He concluded that the key factor of pulse formation is the

attachment process that transforms electrons to negative ions. In the last few years, various numerical simulations of the formation of Trichel pulses have been performed and the above classical viewpoint was accepted in those works [7–11]. However, Trichel pulses can actually be observed in non-electronegative gases such as nitrogen and argon, which cannot be explained by the above theory. Some researchers tried to explain this phenomenon by different mechanisms. Gernak's group [12, 13] observed pulse signals that are very similar to Trichel pulses in non-electronegative gases. They also found that pulse formation does not only depend on negative ions. Akishev *et al* [14] observed Trichel pulses in nitrogen and suggested that the behavior of a positive ion cloud near the cathode provides an explanation for the pulse formation. Ouyang's group [15–18] observed Trichel pulse trains in argon and nitrogen and measured the current–voltage (V – I) curve of the discharge cell under various pressures. Their results suggested the decisive role of positive ions in

* Authors to whom any correspondence should be addressed.

Trichel pulse formation. They found that adding oxygen to the above gases increased the voltage range at which Trichel pulses appear. The team further performed numerical simulations of this phenomenon and found that Trichel pulses could be reproduced when the production rate of negative ions was set to 100%, 1% and 0 [18]. Negative ions indeed affect the pulse amplitude and pulse decay edge, but are not necessary for pulse formation. It is thought that a transient ion sheath consisting of positive ions forms during the temporal discharge, which has an effect on pulse formation. Sun *et al* [19, 20] compared the current pulses in nitrogen and air and found that the pulse rising edge is very similar for pulses in these two gases. They also found that the electronegativity of the working gas affects the pulsed–pulseless mode transition.

Self-pulsing was also observed in parallel-plate DC discharge, usually associated with the negative differential resistivity (NDR) in the subnormal glow mode, which is the transformation between the Townsend and normal glow regimes. Phelps and Petrovic *et al* [21–23] systematically investigated laser-induced and spontaneous oscillations under various conditions. They measured the effect of discharge conditions and external circuit conditions on pulse frequency and oscillation boundaries. They further developed the models of oscillation and NDR behavior of discharges, and obtained the analytic solutions for the time dependence of current and voltage, the angular frequencies, as well as the damped coefficients. They proposed that the large negative differential resistance which represents space-charge distortion of the electric field, capacitance of the external circuit, nonlinear ionization and the feedback process during the pulse discharge leads to the instabilities and oscillations. Petrovic *et al* [24] also studied the spatiotemporal evolution of damped discharge oscillation and found that the discharge can reach the glow mode before being sustained in the Townsend regime. Kuschel *et al* [25] found that low-frequency relaxation and high-frequency free-running oscillations can be produced by changing power supply voltage or discharge current. Huang *et al* [26] found that the rising rate of the voltage has effects on the discharge current rise time and proposed a fluid model which predicted results that agreed well with experiments. He *et al* [27] measured the V – I characteristic of parallel-plate discharge in argon and showed that the V – I curve can be divided into three stages, i.e., Townsend discharge, self-pulsing and normal glow discharge stage. They also built an equivalent circuit model that can reproduce the pulse sequences. Their results confirmed that the self-oscillating of planar discharge can be described by the charging and discharging of a capacitor, which is also similar to a Trichel pulse. Alslanbekov *et al* [28] proposed a discharge model coupling the discharge and external circuit for parallel-plate geometry. They concluded that the circuit is important for the subnormal regime. Levko *et al* [29] obtained the current–voltage characteristics for both planar and curved configurations using a two-dimensional (2D) fluid model. They found that there is an NDR in the subnormal regime, which is characterized by plasma parameter oscillations, and that the self-oscillations are due to the ion transit time instability.

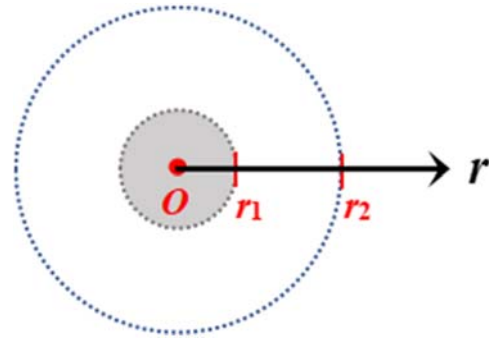


Figure 1. Simulation configuration.

Although the Trichel pulse of corona discharge and the self-pulsing of parallel-plate discharge have been widely studied experimentally and theoretically, their mechanisms still need further investigation. Types of self-pulsing are generally similar, but the pulse phenomenon under different electrode configurations has not been unified.

In this work, we numerically investigated the self-pulsing in DC discharge in argon by a 1D fluid model with the aimed of reproducing the self-pulsing discharge in configurations from corona to parallel-plate within the same framework.

2. Model description

Corona discharges can occur in a wire-to-cylinder configuration, which is actually an axis-symmetric cylinder-to-cylinder 2D discharge. Since the discharge is uniform in the azimuthal direction of the cylindrical coordinate, a 1D discharge channel along the radial direction can describe this corona geometry well, as shown in figure 1. The radii of inner and outer conductive cylinders, r_1 and r_2 , define the boundary of the discharge area; hence, the discharge region is between (r_1, r_2) in simulation and the gas gap is $d = r_2 - r_1$. On the other hand, when r_1 and r_2 are much larger than the gap d , the cylinder-to-cylinder configuration actually turns into a plate-to-plate or parallel-plate one. Then, this 1D model can also describe the traditional parallel-plate discharge.

A negative DC voltage U_0 is applied to the inner cylinder (acting as a cathode) through the ballast resistance R , while the outer one (acting as an anode) is grounded (or the potential at r_2 is zero). The voltage U on the cathode (or the potential at r_1) follows the equation $U = U_0 - IR$ (where I is the discharge current).

We considered in this model two kinds of charged particles, i.e., electrons and positive argon ions. Spatial–temporal behaviors of these charges and the electric field distribution are calculated by solving the coupled continuity equations of charged particles and Poisson’s equation based on the hydrodynamic drift-diffusion approximation as follows,

$$\begin{aligned} \frac{dn_e}{dt} + \frac{1}{r} \frac{\partial}{\partial r} \left(r \left(-\mu_e n_e E_r - D_e \frac{1}{r} \frac{\partial}{\partial r} r n_e \right) \right) \\ = \alpha n_e \mu_e E_r - k_{ep} n_e n_p \end{aligned}$$

Table 1. Swarm parameters.

Parameter	Value	Unit
α	$12p \exp[-180/(E/p)]$	cm^{-1}
γ	0.01	
k_{ep}	2×10^{-6}	$\text{cm}^3 \text{s}^{-1}$
μ_e	$3.3 \times 10^5/p$	$\text{cm}^2 \text{V}^{-1} \text{s}^{-1}$
μ_p	$1.43 \times 10^3/p$	$\text{cm}^2 \text{V}^{-1} \text{s}^{-1}$

Table 2. Boundary conditions.

	Inner	Outer
Ions	$\nabla n_p = 0$	$n_p = 0$
Electrons	$\vec{\Gamma}_e = -\gamma \cdot \vec{\Gamma}_p$	$\nabla n_e = 0$

$$\begin{aligned} \frac{dn_p}{dt} + \frac{1}{r} \frac{\partial}{\partial r} \left(r \left(-\mu_p n_p E_r - D_p \frac{1}{r} \frac{\partial}{\partial r} r n_p \right) \right) \\ = \alpha n_e \mu_e E_r - k_{ep} n_e n_p \\ \frac{1}{r} \frac{\partial}{\partial r} (r E_r) = \frac{e(n_p - n_e)}{\varepsilon}, \end{aligned}$$

where n_e and n_p are the number densities of electron and positive ions, respectively, ε is the gas permittivity, E is the electric field, k_{ep} is the electron-ion recombination coefficients, and α is the ionization coefficient. μ_{ep} and D_{ep} are the mobility and diffusion coefficients of the electron and ion, respectively. The discharge parameter of our model in argon is shown in table 1. The electron-production mechanism is that a high-energy electron collides with a neutral argon atom, ionizing the argon atom to an argon ion Ar^+ and an electron. The electron dissipation mechanism is the recombination of the electrons and argon ions to neutral argon atoms. The mobility and diffusion coefficients of the same species satisfy the Einstein relation,

$$\frac{D_{ep}}{\mu_{ep}} = \frac{k_B T_{ep}}{e}.$$

In this model, a negative voltage is applied to the cathode while the anode is grounded. Therefore, the Dirichlet boundary condition can be used for Poisson's equation. For the continuity equations, generally, the particle density and the flux density of the charged particles at the boundary should be set. The zero-density gradient of ions at the cathode indicates that positive ions move towards the cathode and are all absorbed by the cathode. Positive ions are repelled by the anode, so the density of positive ions at the anode is zero. Positive ions bombard the cathode, which produces a secondary electron flux at the inner boundary. The boundary conditions of the continuity equations are summarized in table 2. A similar setting of boundary conditions was used in [10].

The initial density of the electron and ion is $n_{ep} = 10^4 \text{ cm}^{-3}$. Changeable parameters in this work include the gas pressure p , the radii of inner and outer cylinders (r_1

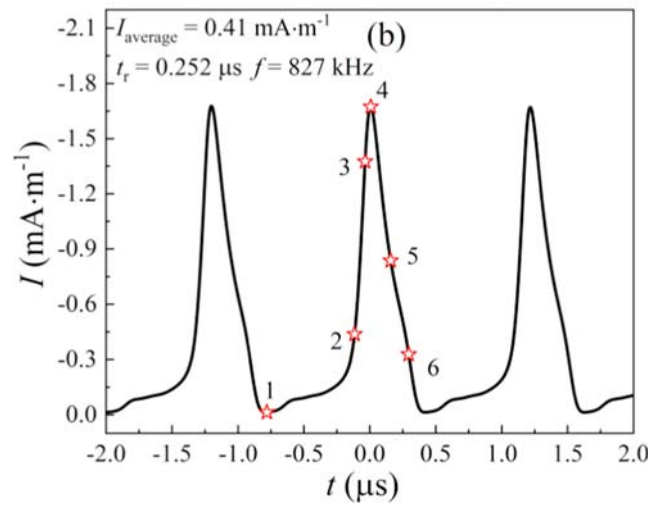
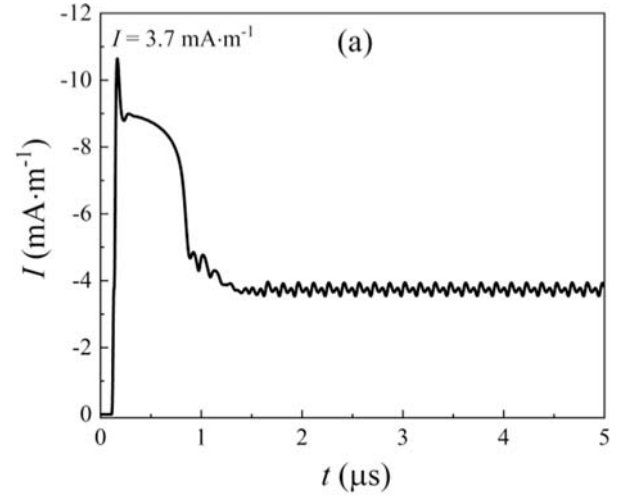


Figure 2. Calculated current of corona discharge in Ar at (a) $U_0 = -1550 \text{ V}$, $R = 20 \text{ k}\Omega$ and (b) $U_0 = -1425 \text{ V}$, $R = 300 \text{ k}\Omega$ ($r_1 = 0.05 \text{ mm}$, $d = 5 \text{ mm}$, $p = 190 \text{ Torr}$).

and r_2), the ballast resistor R , and the applied negative voltage U_0 .

3. Results and discussion

3.1. Validity of the model

Firstly, the model validation was performed. For that, we calculated the discharge current in a corona configuration. This can be achieved by setting a small inner radius $r_1 = 0.05 \text{ mm}$ and a large outer radius $r_2 = 5.05 \text{ mm}$ so that r_1 is much smaller than the gap $d = 5 \text{ mm}$.

Figure 2 shows the calculated discharge current for $U_0 = -1550 \text{ V}$ and 1425 V . The gas pressure is $p = 190 \text{ Torr}$. It is shown that when $U_0 = -1550 \text{ V}$ is applied, the discharge current increases to the peak, then decreases and tends to be stable around $I = 3.7 \text{ mA m}^{-1}$. This is similar to the development process of glow discharge [30]. When a lower voltage $U_0 = 1425 \text{ V}$ is applied, the current is pulsed. The averaged current is $\sim 0.41 \text{ mA m}^{-1}$, the pulse rising time is

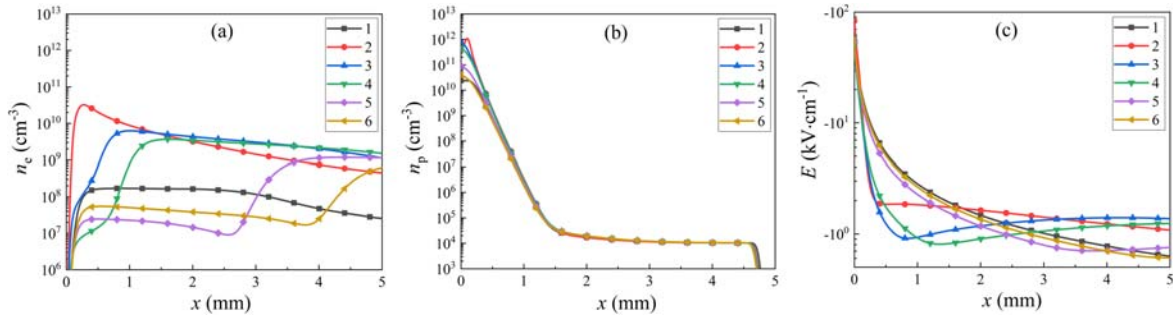


Figure 3. Distributions of (a) electron density, (b) positive ion density and (c) electric field of corona discharge at various times (corresponding to t_1 – t_6 in figure 2(b)). Discharge conditions are shown in figure 2(b).

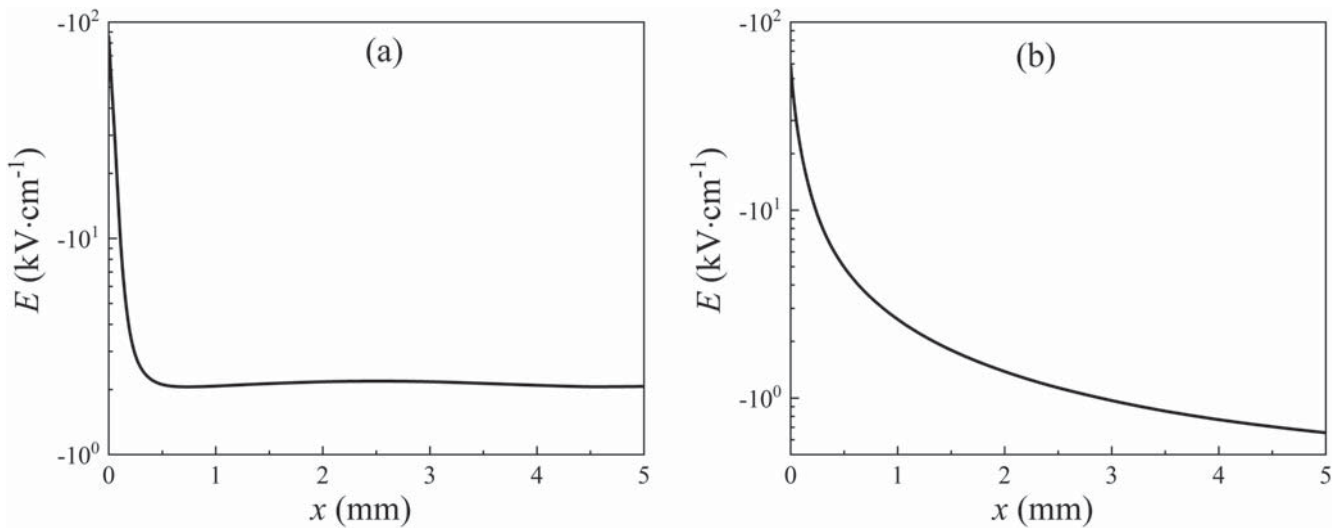


Figure 4. Distributions of electric field for (a) normal glow discharge at $U_0 = 1590$ V, $R = 20$ k Ω and (b) Townsend discharge at $U_0 = 1430$ V, $R = 500$ k Ω in the corona configuration.

$t_r = 252$ ns and the pulse interval time is 1209 ns, corresponding to a repetition frequency of $f = 827$ kHz. The pulsed characteristics are generally similar to a Trichel pulse and the current waveform is acceptable [1, 2]. This indicates that the present model can well reproduce the breakdown and discharge processes observed by the experiment; hence, it should be valid for investigating discharge characteristics.

3.2. Self-pulsing in a corona configuration

We now investigate the pulsed discharge process in the above corona structure. Figure 3 shows the time-resolved particle density in space at various times and the electric field intensity distribution along the discharge gap at each time marked by ‘stars’ in figure 2 (t_1 – $t_6 = -0.7795, -0.1205, -0.0385, 0, 0.1715$ and 0.291 μ s). The cathode surface of ($r = r_1$) is defined as $x = r - r_1 = 0$, and so on in the rest of the article.

There are some electrons in the space due to the Townsend mode with a very weak current. At the beginning of the pulsed discharge, the electron density increases near the cathode region, accompanied by a rise in current (see t_1 – t_2). Then, many electrons move toward the anode. Meanwhile, the electric field is strongly distorted, with a large intensity in a narrow region near the cathode ($x \lesssim 1$ mm) and a smaller intensity near the

anode ($x > 1$ mm), indicating the formation of a positive column (see t_3 – t_4). This field structure is very different from the initial state of Townsend discharge, but just like that found in a stable glow discharge (shown below in figure 4(a)). This state cannot be sustained for long and it is soon followed by a decrease in current and electron density in space. Then the field distribution returns to the initial state (see t_5 – t_6), similar to that of Townsend discharge (shown in figure 4(b)).

Figure 4 also shows that in glow discharge, there is a region with a strong field near the cathode ($x \lesssim 0.5$ mm), corresponding to the sheath; while, elsewhere, the field is weak and uniform. In Townsend discharge, the field decreases more gently from the cathode to the anode, which is not significantly different from the initially applied field.

The averaged number density of charged particles over the whole discharge space (shown in figure 5) has a similar oscillation to the current curve in figure 3. The dominant space charges are positive ions, the number density of which is generally one order higher than that of the electrons.

We noticed in the simulation that the lowest and the highest current densities for the appearance of self-pulsing are 0.128 mA m^{-1} and 3.8 mA m^{-1} in this corona configuration. The current limits for stable Townsend and glow discharge are much different. Discharge between Townsend and glow

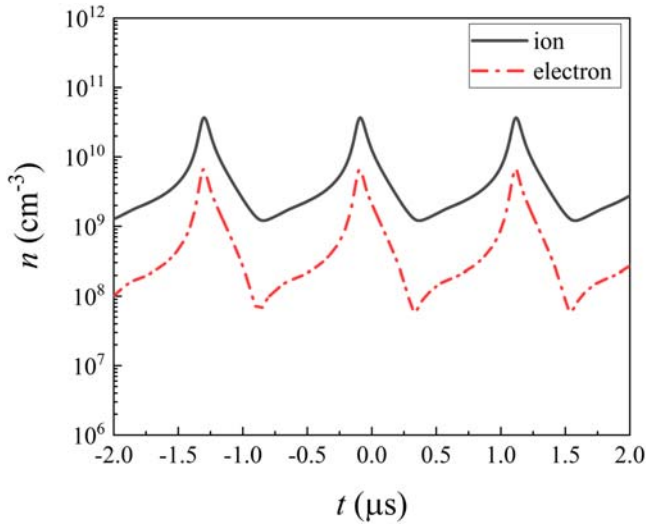


Figure 5. Variation of the number density of space charges with time. Discharge conditions are in figure 2(b).

discharge is always pulsed. In other words, the appearance of self-pulsing is mainly affected by the average discharge current. The discharge is pulsed only when the current is in an appropriate range. The discharge current can be altered either by changing the applied voltage U_0 or by the ballast resistance R . However, the external circuit does not dominate the appearance of self-pulsing, although the value of R has an influence on the pulsing characteristics. This is in agreement with the previous experimental and simulated results, e.g., in [27, 29].

The number density of charges at different positions also shows a similar oscillation, as shown in figure 6 for $x = 0.2, 0.5$ and 1 mm. Near the cathode ($x = 0.2$ mm, figure 6(a)), the positive ions are dominant, but the density of positive ions drops dramatically by one to three orders of magnitude a little further from the cathode surface ($x = 0.5$ mm) or even by five orders of magnitude farther from the cathode ($x = 1$ mm). The electrons, however, do not change significantly in density. They become dominant gradually away from the cathode, as shown in figures 6(b) and (c). This also indicates that the region near the cathode ($x < 0.5$ mm) with a higher density of positive ions is more important for pulsing discharge.

3.3. Self-pulsing in a parallel-plate configuration

In the case of large inner and outer radii r_1 and r_2 , the system is actually a parallel-plate configuration. In this case, there are three discharge modes, i.e., stable Townsend discharge of low current density, stable glow discharge of high current and pulsed discharge between them.

Figure 7 shows the pulsed waveform for this planar discharge in argon with $r_1 = 50$ mm, $r_2 = 51$ mm (hence $d = 1$ mm), $U_0 = -1280$ V, $R = 2$ k Ω and $p = 190$ Torr. Under these conditions, the averaged current in simulation is $I_{\text{average}} = 111.4$ mA m^{-1} , the pulse rising time is $t_r = 0.6775$ μs and the pulse frequency is $f = 802$ kHz. When the current density is lower than 96.8 mA m^{-1} , or higher than 115.8 mA m^{-1} , discharge is stable in the Townsend or glow regime, respectively. A stable subnormal mode [28, 29] cannot be

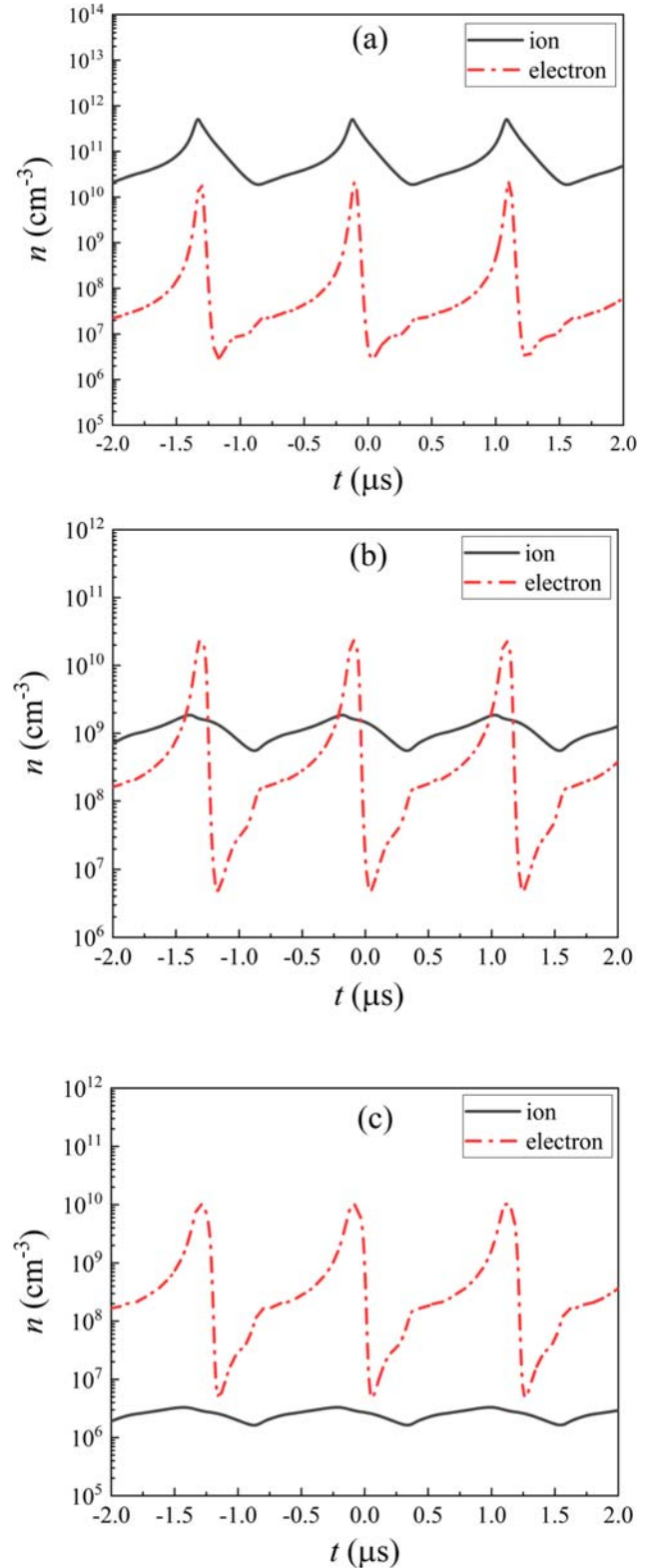


Figure 6. Charge number density versus time at (a) $x = 0.2$ mm, (b) $x = 0.5$ mm and (c) $x = 1$ mm with time. Discharge conditions are the same as those in figure 2(b).

obtained in this simulation (also in the corona configuration), although the averaged current density is that of subnormal glow.

Figure 8 is the distribution of time-resolved electron, ion density and electric field along the gap at various times

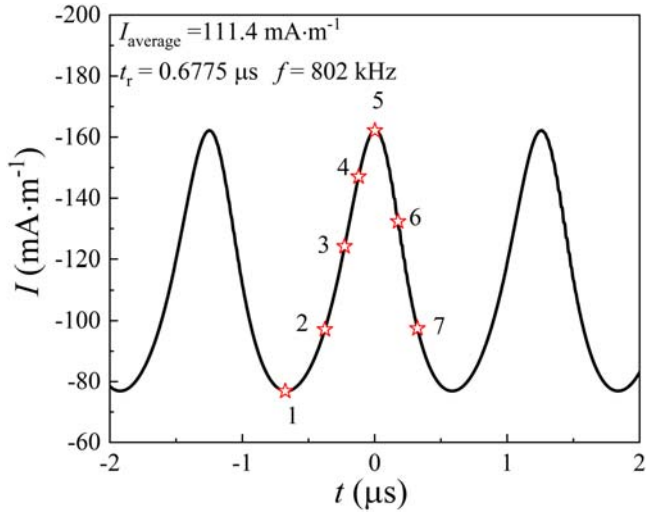


Figure 7. Current waveform of self-pulsing in a parallel-plate configuration in Ar ($r_1 = 50$ mm, $r_2 = 51$ mm ($d = 1$ mm), $p = 190$ Torr, $U_0 = 1280$ V, $R = 2$ k Ω).

marked by ‘stars’ 1–8 in figure 7 (i.e., t_1 – $t_7 = -0.7795$, -0.4855 , -0.3345 , -0.2185 , 0 , 0.1785 and 0.3320 μ s).

Initially, there are a few electrons in the space caused by the weak Townsend discharge (see t_1 – t_2). With the increase of discharge current, ions grow quickly in the near-cathode regions, forming a sheath-like layer of a higher electric field ($x \lesssim 0.3$ mm). Electrons near the anode increase significantly in density; while ions decrease in density there, forming a positive column-like region ($x > 0.5$ mm) of a lower and roughly constant field (see t_3 – t_5). This indicates a glow mode, showing a distinction from the Townsend mode. However, this temporal glow structure cannot sustain stability and is followed by a decrease of current and electron density in space. The distributions of the field and charge distribution gradually return to the initial state of Townsend discharge (see t_7).

Notice that the field structure in parallel-plate discharge is very different from that in corona. This is due to the different parameters of the two configurations. The curvature radius of the cathode changes the distribution of the electric field significantly.

Similar to pulsed corona discharge, the averaged number density of charged particles over the whole discharge space oscillates with time, as shown in figure 9. In parallel-plate discharge, the dominant charges are also positive ions, the number density of which is generally one order higher than that of the electrons. It should be noticed that the total positive ion density is one order higher than that of electrons for both configurations. This is because the ionic current is higher than the electronic current in most of the discharge space in Townsend (dark) discharge mode. Since the mobility of electrons is much greater than that of positive ions, the difference is even greater in charge densities. In self-pulsing discharge, there is always a background current of Townsend mode (since the pulsed discharge starts from Townsend discharge), so the density of total positive ions is much higher than that of electrons [31].

Considering the local charges in the discharge gap, the number density also shows a similar oscillation, as shown in

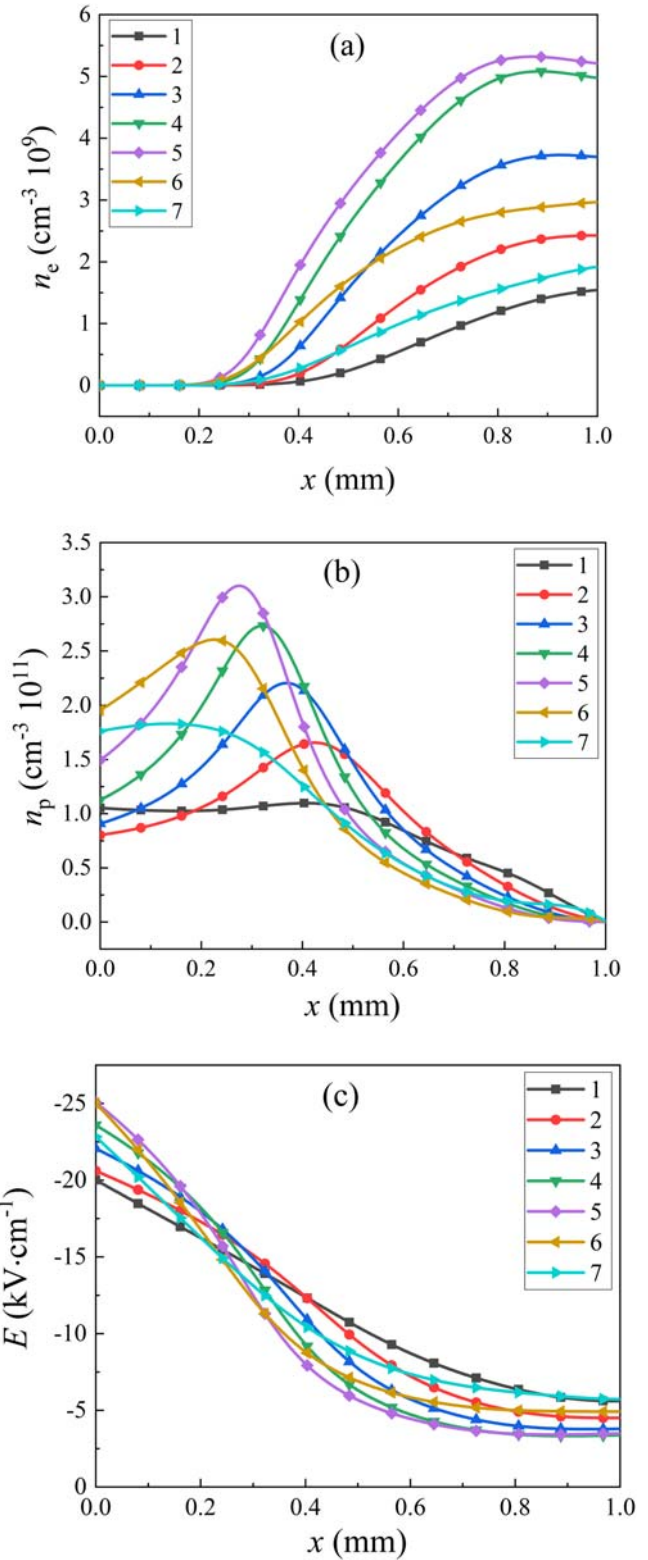


Figure 8. Distributions of (a) electron number density, (b) ion density and (c) electric field of parallel-plate discharge at various times of t_1 – t_7 . Discharge conditions are the same as those in figure 7.

figure 10. In the near-cathode, the dominant charges are ions. The oscillation of these positive ions behind the ion sheath deviates from that of the discharge current (seen in figures 7(b) and (c)), corresponding to cathode sheath formation and dissipation caused by the positive ion. Different from that in

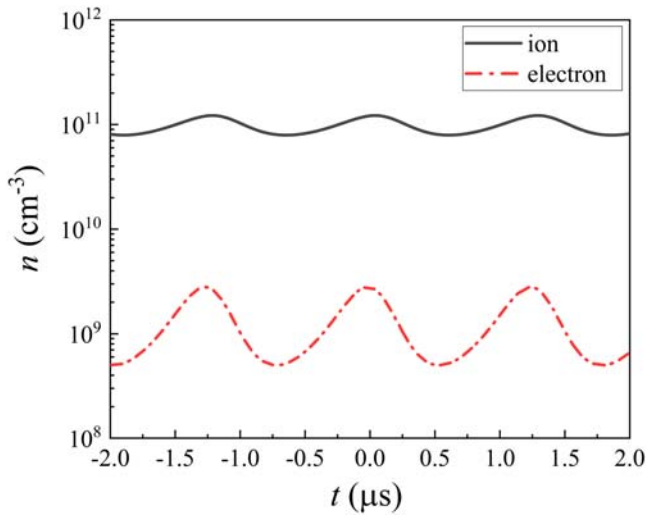


Figure 9. Number density of space charges versus time. Discharge conditions are the same as those in figure 7.

corona discharge, there seems to be a background charge of positive ions in the gap of parallel-plate discharge, in which the electrons oscillate with time. The electrons are only dominant at a position very close to the anode ($x > 0.99$ mm).

3.4. Effect of operation parameters on self-pulsing

3.4.1. Repetition frequency. Figure 11 shows the pulse frequency in argon as a function of the average discharge current under different radii of the cathode. The dots in figure 11 are the frequency of self-pulsing obtained by the simulation at different applied voltages (and thus different discharge currents). The solid lines in figure 11 are used to guide the eyes.

Generally, the average current has significant effects on the pulse characteristics during the self-pulsing phase. It can be seen that the pulsing frequency increases linearly as the discharge current rises. The smaller the cathode radius is, the higher the pulse frequency is. This result is in good agreement with experimental results [17, 30, 32, 33]. However, the pulsed current waveform keeps nearly unchanged as the magnitude increases.

The radius of the cathode curvature directly affects the electric field distribution. The smaller the radius is, the steeper the electric field near the cathode changes, and vice versa, which has effects on the space behaviors of ions during the discharge, and hence the transformation between Townsend and temporal glow regime during the current pulse. In our simulation, the positive ion dissipation is caused mainly by electron–ion recombination, diffusion as well as drift in the electric field. Since the recombination coefficient, diffusion coefficient and ion mobility are set as constants in the model, then the decay of the pulse should be mainly determined by the electric field, which relates to the space charges.

3.4.2. Rising time. Figure 12 shows the rising time of self-pulsing in argon as a function of the average current under different radii of the cathode. The dots in figure 12 are the rising

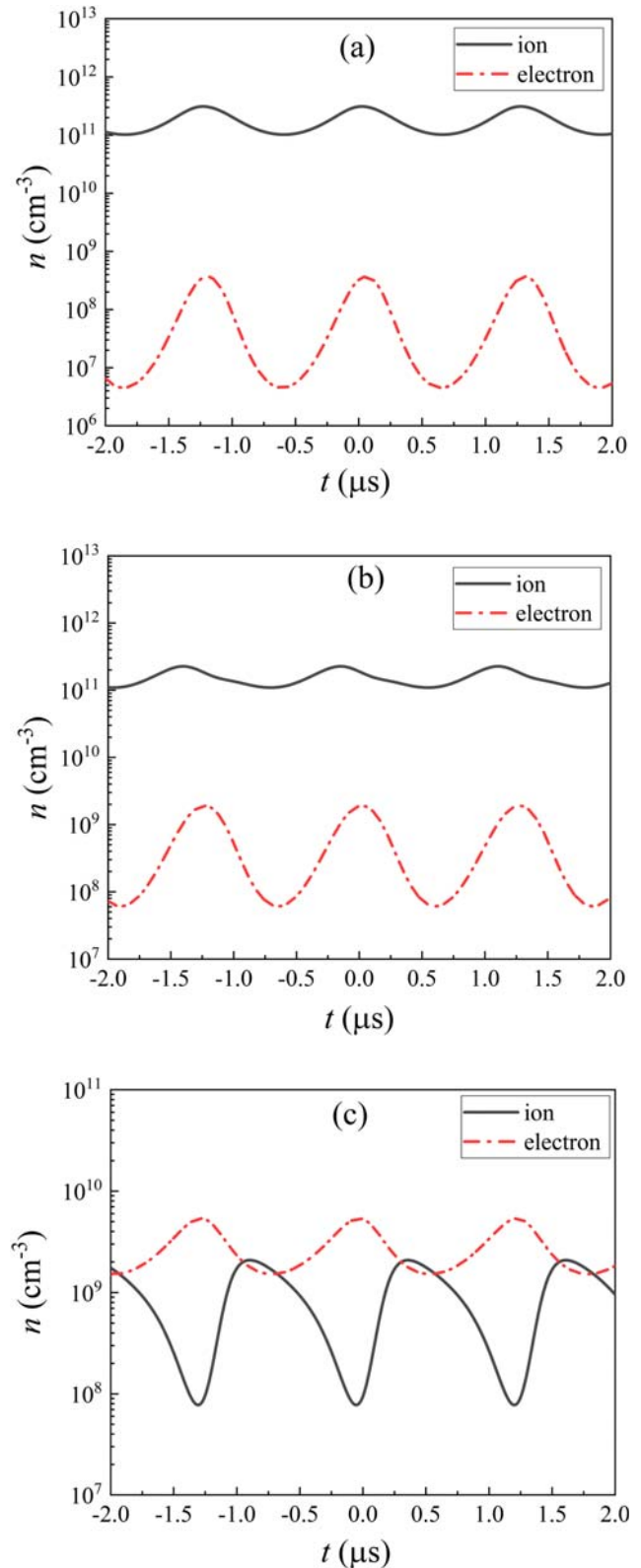


Figure 10. Local charge density versus time at (a) $x = 0.3$ mm, (b) $x = 0.4$ mm and (c) $x = 0.99$ mm with time. Discharge conditions are the same as those in figure 7.

time of the current pulse obtained by the simulation at different applied voltages (and hence different discharge currents).

As seen in figure 12, the rising time increases with the radius of cathode curvature, which is in agreement with the

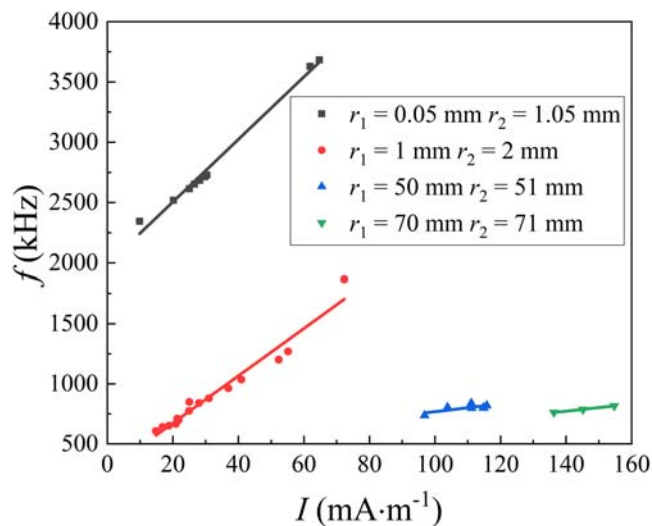


Figure 11. Pulsing frequency as a function of average current under different configurations.

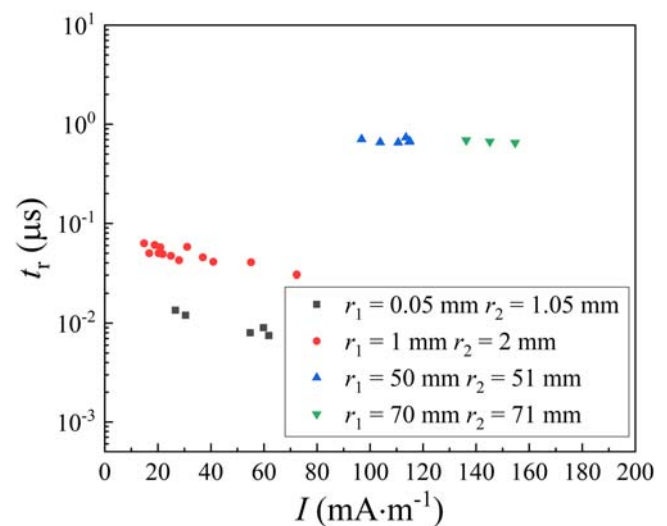


Figure 12. Rising time as a function of average current under different configurations.

previous results [11, 17, 18, 24, 32]. However, the pulse rising time remains nearly unchanged with the discharge current increasing. This is due to the pulse rising edge corresponding to the formation process of the transient glow discharge, the development time of which is not affected by the discharge current. This tendency accords with that found in experiments [11, 24].

However, in the configuration of $r_1 = 50$ and 70 mm, the rising time is nearly the same. This is reasonable since the two configurations are parallel-plate-like.

4. Discussions

As seen above, we reproduced the self-pulsing phenomenon in both corona and parallel-plate configurations with the same model by changing the operating parameters. The pulsing currents generally show similar characteristics, including the current waveform, the discharge development process and their change with the operating conditions. The pulsed discharge is indeed a transition between normal glow and Townsend discharge. The oscillation of the total charged particles in space and local charges at different positions in the discharge gap indicates that the periodic behavior of charges reflects the transition of the discharge mode.

4.1. Formation of the current pulse

The spatial-temporal developments of the pulses show that the formation process of the pulse is that of transient glow discharge. Particularly, the discharge is not extinguished during the pulse interval time but stays in the weak discharge mode of the Townsend regime. The formation of temporal glow discharge is accompanied by the formation of the temporal sheath. At the beginning of the pulse, the discharge initiates in the Townsend regime. As the discharge becomes more intense, the ionization process is significantly enhanced, producing numerous positive ions. Such a great number of

newly produced positive ions cannot be balanced by the drift process and so the charges begin to accumulate in the discharge gap, causing the formation of a transient cathode ion sheath. Finally, when the electric field distortion by space charges becomes strong enough, the temporal cathode sheath and, hence, the glow discharge form.

During this period, negative ions are dispensable. The generation of negative ions does not affect the development of discharge. Indeed, the pulse rising edge is irrelevant to the negative ions [13, 18].

Although the distributions of the electric field and the space charges are very different in corona and parallel-plate configurations, the formation process of the pulsed discharge is nearly the same. It is therefore suggested that the formation mechanism should be the same in the two configurations.

4.2. Decay of current

However, even at the pulse peak time, the discharge current is still too small to sustain an ion sheath and a temporal glow mode would not be sustained stably. Eventually, the positive ion cloud is destroyed by the drift, diffusion and recombination processes; hence, the discharge decays to the weak-current Townsend mode. The pulse interval is dominated by the enhancement of the local electric field so that the temporal glow mode can be formed again. This is actually the re-building of the cathode ion sheath.

Although negative ions are dispensable for the pulse formation, they accelerate the decay of electrons by the attachment process. The presence of negative ions influences the electric field distribution in the space and hence the pulsing characteristics [10].

4.3. Discontinuous transition between Townsend and glow discharge

Low-current Townsend discharge can be maintained steadily when the discharge current is large enough for self-sustained

discharge but also weak enough so that the accumulation of positive ions in the discharge gap does not distort the applied electric field significantly. However, the Townsend mode becomes unstable if the current reaches a critical value (the upper limit, say $I_{TS,up}$). From the above results, the minimum current in this simulation is 10 mA for $r_1 = 0.05$ mm and 136 mA m^{-1} for $r_1 = 70$ mm. On the other hand, normal glow discharge can only be sustained at high current density because the formation of a sheath structure needs high current density. This critical value (or the lower limit, $I_{GD,low}$) in the above calculated conditions is about 65 mA m^{-1} for $r_1 = 0.05$ mm and 155 mA m^{-1} for $r_1 = 70$ mm. Clearly, $I_{GD,low} \gg I_{TS,up}$, hence the discharge would not transform continuously between each other. Pulsed discharge occurs when the mode transits. There is no stable subnormal stage between the two stable discharges, although the averaged current density of the pulsed current is of subnormal glow. Only when the minimum current for a stable glow mode is not significantly greater than the upper limit for the stable Townsend regime can the ‘quasi-glow discharge’ phase with negative differential resistance be achieved, like in [28, 29].

The formation mechanism of self-pulsing discharge for both configurations is the same. It is caused by the mode transition between the instantaneous glow mode and the Townsend mode, despite the differences in the distributions of space charge and electric field. This self-pulsing seems to be different from the subnormal mode (e.g., mentioned in [28, 29]). The pulsed stage is due to the intrinsic feature of the DC discharge itself, in both corona and parallel-plate configurations, rather than the external circuit, which occurs when $I_{GD,low} \gg I_{TS,up}$. Indeed, the external circuit may have some influence on the formation of a stable subnormal mode [28, 29] as well as the characteristics of self-pulsing [27, 29], but it is not involved in the formation mechanism of the pulse.

The above results do not depend on the working gas; hence, in principle, self-pulsing might occur in any gas if the conditions are suitable.

5. Conclusion


We developed a unified 1D fluid model to investigate the self-pulsing phenomenon in negative corona and/or parallel-plate discharge in argon. This oscillation has similar instabilities in various configurations and various gases, which depends on the current density. They always appear between the stable discharge modes of the small-current Townsend regime and the large-current normal glow regime. Self-pulsing discharge appears when a discontinuous transition between them occurs. The pulse rising edge is associated with the formation process of the temporal glow mode, which is determined by the formation of a temporal ion sheath or cloud. The decay of the pulsed discharge is associated with the dissipation of the transient cathode sheath due to the decay of positive ions. The

interval of two pulses is dominated by the re-building of the cathode ion sheath.

Acknowledgments

This work was supported in part by the Electrostatic Research Foundation of Liu Shanghe Academicians and Experts Workstation, Beijing Orient Institute of Measurement and Test (No. BOIMTLSHJD20221002).

ORCID iDs

Jiting OUYANG (欧阳吉庭)  <https://orcid.org/0000-0002-0236-9886>

References

- [1] Trichel G W 1938 *Phys. Rev.* **54** 1078
- [2] Van Brunt R J and Leep D 1981 *J. Appl. Phys.* **52** 6588
- [3] Gardiner P S, Moruzzi J L and Craggs J D 1978 *J. Phys. D: Appl. Phys.* **11** 237
- [4] Gardiner P S and Craggs T D 1977 *J. Phys. D: Appl. Phys.* **10** 1003
- [5] Morrow R 1985 *Phys. Rev. A* **32** 1799
- [6] Morrow R 1985 *Phys. Rev. A* **32** 3821
- [7] Guo Y L *et al* 2021 *AIP Adv.* **11** 125107
- [8] Lu B X and Song L J 2021 *AIP Adv.* **11** 085013
- [9] Salah W S *et al* 2022 *AIP Adv.* **12** 105123
- [10] Gao Q Q *et al* 2020 *Phys. Plasmas* **27** 113508
- [11] Zheng Y S *et al* 2017 *Phys. Plasmas* **24** 063515
- [12] Černák M and Hosokawa T 1988 *Appl. Phys. Lett.* **52** 185
- [13] Černák M *et al* 1998 *J. Appl. Phys.* **83** 5678
- [14] Akishev Y S *et al* 2001 *Plasma Phys. Rep.* **27** 520
- [15] Zhang Y *et al* 2017 *Sci. Rep.* **7** 10135
- [16] Zhang Y *et al* 2016 *J. Phys. D: Appl. Phys.* **49** 245206
- [17] Xia Q *et al* 2018 *Phys. Plasmas* **25** 023506
- [18] Xia Q *et al* 2017 *J. Phys. D: Appl. Phys.* **50** 505205
- [19] Zhang X *et al* 2020 *Phys. Plasmas* **27** 033501
- [20] Zhang X *et al* 2021 *Phys. Plasmas* **28** 063505
- [21] Phelps A V, Petrović Z L and Jelenković B M 1993 *Phys. Rev. E* **47** 2825
- [22] Petrović Z L and Phelps A V 1993 *Phys. Rev. E* **47** 2806
- [23] Jelenković B M, Rózsa K and Phelps A V 1993 *Phys. Rev. E* **47** 2816
- [24] Marić D, Malović G and Petrović Z L 2009 *Plasma Sources Sci. Technol.* **18** 034009
- [25] Stefanović I *et al* 2011 *J. Appl. Phys.* **110** 083310
- [26] Huang B D *et al* 2015 *J. Phys. D: Appl. Phys.* **48** 125202
- [27] He S J *et al* 2020 *J. Appl. Phys.* **127** 213302
- [28] Arslanbekov R R and Kolobov V I 2003 *J. Phys. D: Appl. Phys.* **36** 2986
- [29] Levko D and Raja L L 2021 *J. Phys. D: Appl. Phys.* **54** 235201
- [30] Zhang L J *et al* 2022 *IEEE Trans. Power Deliv.* **37** 3792
- [31] Raizer Y P 1991 *Gas Discharge Physics* (Berlin: Springer)
- [32] Zhang Y *et al* 2015 *J. Electr. Eng. Technol.* **10** 1174
- [33] Lama W L and Gallo C F 1974 *J. Appl. Phys.* **45** 103